

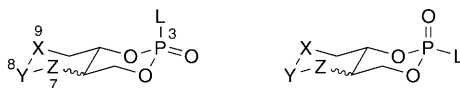
3-Fluoro-2,4-dioxa-7-aza-3-phosphadecalin 3-Oxides as Rigid Acetylcholine Mimetics: Conformational Analysis and Direct Evidence of the Anomeric Effect

by Stefan Furegati, Martin Binder, Anthony Linden, and Peter Ruedi*

Organisch-chemisches Institut der Universität Zürich, Winterthurerstrasse 190, CH-8057 Zürich

Conformational analyses of the P(3)-axially and P(3)-equatorially F-substituted (\pm)-*cis*- and (\pm)-*trans*-2,4-dioxa-7-aza-3-phosphadecalin 3-oxides (3-fluoro-2,4-dioxa-7-aza-3-phosphabicyclo[4.4.0]decane 3-oxides) were performed. The results are based on independent studies in both solution and the solid state by ^1H - and ^{31}P -NMR experiments and computational and X-ray crystallographic data. As expected, the axial epimers adopt neat double-chair conformations in solution and in the crystal. Due to the anomeric effect of the electron withdrawing F-substituent, the 2,4-dioxa-3-phospha moiety in the equatorial epimers adopts a mixture of conformations in solution, mainly chair and twist-boat; whereas a neat twist-boat (*trans*-isomer) and the unusual envelope conformation (*cis*-isomer) were detected in the solid state. This is the first report of a straight visualization of these conformations and the impact of the anomeric effect in such systems.

1. Introduction. – In a recent paper [1], we have reported on the synthesis and characterization of 3-substituted, *cis*- and *trans*-2,4-dioxa-9-aza- (**I**), 2,4-dioxa-8-aza- (**II**), and 2,4-dioxa-7-aza-3-phosphabicyclo[4.4.0]decane 3-oxides (**III**) (Fig. 1). The novel heterocycles are configuratively fixed and conformationally constrained P-analogues of acetylcholine (7-aza- and 9-aza isomers) or γ -homo-acetylcholine mimetics (8-aza isomers). Being inhibitors of acetylcholinesterase (AChE) [2], the compounds are considered to be suitable probes for the investigation of molecular interactions with the enzyme, such as the recognition conformation of acetylcholine (ACh) and the stereochemistry of the inhibition reaction.



- I** X = NR, NR₂[⊕], Y = Z = CH₂
II X = CH₂, Y = NR, NR₂[⊕], Z = CH₂
III X = Y = CH₂, Z = NR, NR₂[⊕]
IV X = Y = Z = CH₂

L = electron-withdrawing group
(F, Cl, N₃, OR, NR₂, SR)

Fig. 1. The 2,4-dioxa-3-phosphadecalins of types **I–IV**

The ^{31}P -NMR spectroscopic data of these novel compounds are most informative and allow structural assignments such as the relative configuration at the P-atom and the conformation of the 2,4-dioxa-3-phospha moiety. In this report, we present conformational analyses of the (\pm)-3-fluoro-2,4-dioxa-7-aza-3-phosphabicyclo[4.4.0]decane 3-oxides (= 2-fluorohexahydro-4*H*-1,3,2-dioxaphosphorino[5,4-*b*]pyridine 2-oxides) **1ax**, **1eq**, **2ax**, and **2eq** (Fig. 2; type **III** [1]). The results are based on the ^{31}P -NMR chemical shifts, ^{31}P , ^1H -coupling data, and the crucial role played by the anomeric effect [3]. Moreover, the conformational impacts of the latter are directly visualized for the first time by virtue of X-ray crystallographic analyses. A knowledge of the decisive conformations is a prerequisite for the rationalization of the stereochemical course of nucleophilic displacement reactions at the P-atom, in particular the inhibition of the serine hydrolases chymotrypsin [4–6] and AChE [7].

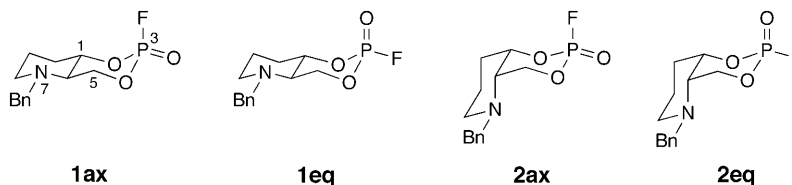


Fig. 2. The isomeric 3-fluoro-2,4-dioxa-7-aza-3-phosphadecalins **1** and **2**

2. ^{31}P -NMR Spectroscopic Properties: the Relative Configuration at the P-atom. –

2.1. *The Chemical Shift.* According to generalized stereoelectronic considerations [8][9], the ^{31}P -NMR chemical shifts are dependent on the P–O ester dihedral angles. Calculations indicate that a phosphate diester in a *gauche,gauche* conformation would have a chemical shift substantially upfield from that of a phosphate ester in more extended conformations such as *gauche,trans* or *trans,trans* (*trans* = *anti*-periplanar) [10]¹⁾. Experimentally, the stereoelectronic effect on ^{31}P -NMR chemical shifts can be confirmed by using six-membered-ring systems in which the torsional angles are rigidly defined by some molecular constraint. The 2,4-dioxa-3-phosphadecalins **I–IV** (Fig. 1) ideally meet these requirements, and the ^{31}P -NMR resonance of the axial P(3)-epimers is expected to be diamagnetically shifted with respect to their equatorially substituted counterparts.

2.2. *The Coupling Pattern.* The magnitude of the vicinal $J(\text{P},\text{H})$ is dependent on the P–O–C–H dihedral angle (Φ) and exhibits a maximum value at 180° and a broad minimum at *ca.* 90° (modified *Karplus* equation) [8][10]. Therefore, the splitting pattern is indicative of the conformations present in cyclic phosphates: in particular, in the chair conformation of the 2,4-dioxa-3-phospha moiety, only $\text{H}_{\text{eq}}-\text{C}(5)$ has $\Phi = 180^\circ$ which results in a large coupling ($^3J(\text{P},\text{H}) \approx 25$ Hz), whereas $\text{H}-\text{C}(1)$ and $\text{H}_{\text{ax}}-\text{C}(5)$ have

¹⁾ In the phosphoric acid esters with a cyclic 2,4-dioxa-3-phospha structure, the bond angles are significantly distorted from tetrahedral values, and this distortion is more pronounced in the equatorially substituted P-epimers. In these compounds the ester P–O bond angles contract to *ca.* 103° , while the ester P=O angles increase to *ca.* 115° . This variation from tetrahedral symmetry results in a hybridization change on the P-atom which is quite likely responsible for the diamagnetic ^{31}P -NMR chemical shifts of these epimers [11].

$\Phi = 60^\circ$ and show only very small couplings (${}^3J(\text{P,H}) \approx 0-1$ Hz). Hence, a pseudo-*d* is observed in the ${}^{31}\text{P}$ -NMR spectrum. In other conformations, as $\Phi(\text{P,H}_{\text{eq}}-\text{C}(5))$ decreases and $\Phi(\text{P,H}_{\text{ax}}-\text{C}(5))$ and $\Phi(\text{P,H}-\text{C}(1))$ increase, the ${}^{31}\text{P}$ -NMR spectra exhibit complex multiplicities.

2.3. The Relative Configuration at the P-Atom. As discussed above, the interpretation of both chemical-shift and coupling data enable the assignment of the relative configuration at the P-atom in the 2,4-dioxa-3-phosphadecalins. In the course of our investigations, we observed that in the 3-epimer pairs of compounds **I–IV**, the upfield $\delta(\text{P})$ is generally accompanied by a *d*-like signal with ${}^3J(\text{P,H}) \approx 25$ Hz. Consequently, axial substitution at P(3) was assigned to these compounds, whereas the paramagnetically shifted *m* signals were attributed to the equatorial P-epimers. By comparing various P-substituents (Fig. 1), the magnitude of the chemical shift difference ($\Delta\delta = \delta_{\text{eq}} - \delta_{\text{ax}}$) was shown to be inversely proportional to the electronegativity of the P-substituent; we found a typical range from *ca.* 0.5 (L=F) to 7 ppm (L=S), *i.e.*, $\Delta\delta > 0$ [1][4][5][12]. However, the cyclic phosphorofluoridates of the *cis*-series of the type **I–IV** compounds (L=F) do not follow this empirical rule and display an inverse behavior ($\Delta\delta \leq 0$). From this result, it could be anticipated that the strongly electron-withdrawing F-substituent occupies an axial position in both diastereoisomers, a fact that can only be explained by significant conformational changes.

3. Conformational Analysis in Solution: the Anomeric Effect. – 3.1. *General.* As outlined above, the ${}^1\text{H}$ -coupled ${}^{31}\text{P}$ -NMR spectra constitute a valuable probe for the conformational analysis of our cyclic phosphorofluoridates (Fig. 3): The *d*-like high-field signals clearly indicate the chair conformation of the 2,4-dioxa-3-phospha moiety in the axial epimers. In contrast, the corresponding low-field resonances exhibit complex multiplicities, *i.e.*, the equatorial counterparts do not adopt the sterically favored chair conformation. This can be explained by the anomeric preference for placing electronegative substituents in the axial rather than in the equatorial position [3][9]. By flipping from the chair to a boat or a twist-boat conformation, the equatorial ester bond moves into a (pseudo)axial position. The resulting minimum-energy conformation represents a balance between the anomeric effect favoring the axial orientation in distorted conformations and the 1,3-steric and -eclipsing interactions favoring the chair conformation.

3.2. ${}^{31}\text{P}$, ${}^1\text{H}$ -NMR Spectra. – 3.2.1. *The Modified Karplus Equation; the Axial Epimers 1ax and 2ax.* Since any deviation from a *d*-like multiplicity (Fig. 3) is indicative of the existence of nonchair conformations, the interpretation of the ${}^3J(\text{P,H})$ -pattern allows an assignment of the dihedral angles (Φ) and, as a consequence, the assignment of the conformation adopted by the respective compound in solution.

The double-chair conformation of the P(3)-axially substituted decalins **1ax** and **2ax** is sterically and stereoelectronically favored²⁾). Hence, it can be anticipated that the conformation in solution corresponds with that in the crystal structure. Based on the

²⁾ The ${}^3J(\text{P,H})$ values are based on ${}^{31}\text{P}$ -, ${}^1\text{H}$ -, and ${}^1\text{H}\{{}^{31}\text{P}\}$ -NMR spectra [1]. The additional splitting in **2ax** (7.5 Hz, Fig. 3) was unambiguously assigned to ${}^4J(\text{P,H}_{\text{ax}}-\text{C}(10))$ by ${}^1\text{H}\{{}^{31}\text{P}\}$ -NMR experiments.

³⁾ The fully ring-inverted double chair that is always possible in the *cis*-decalins, **C-2**, is strongly disfavored (equatorial F-substituent) and need not be considered for **2ax**.

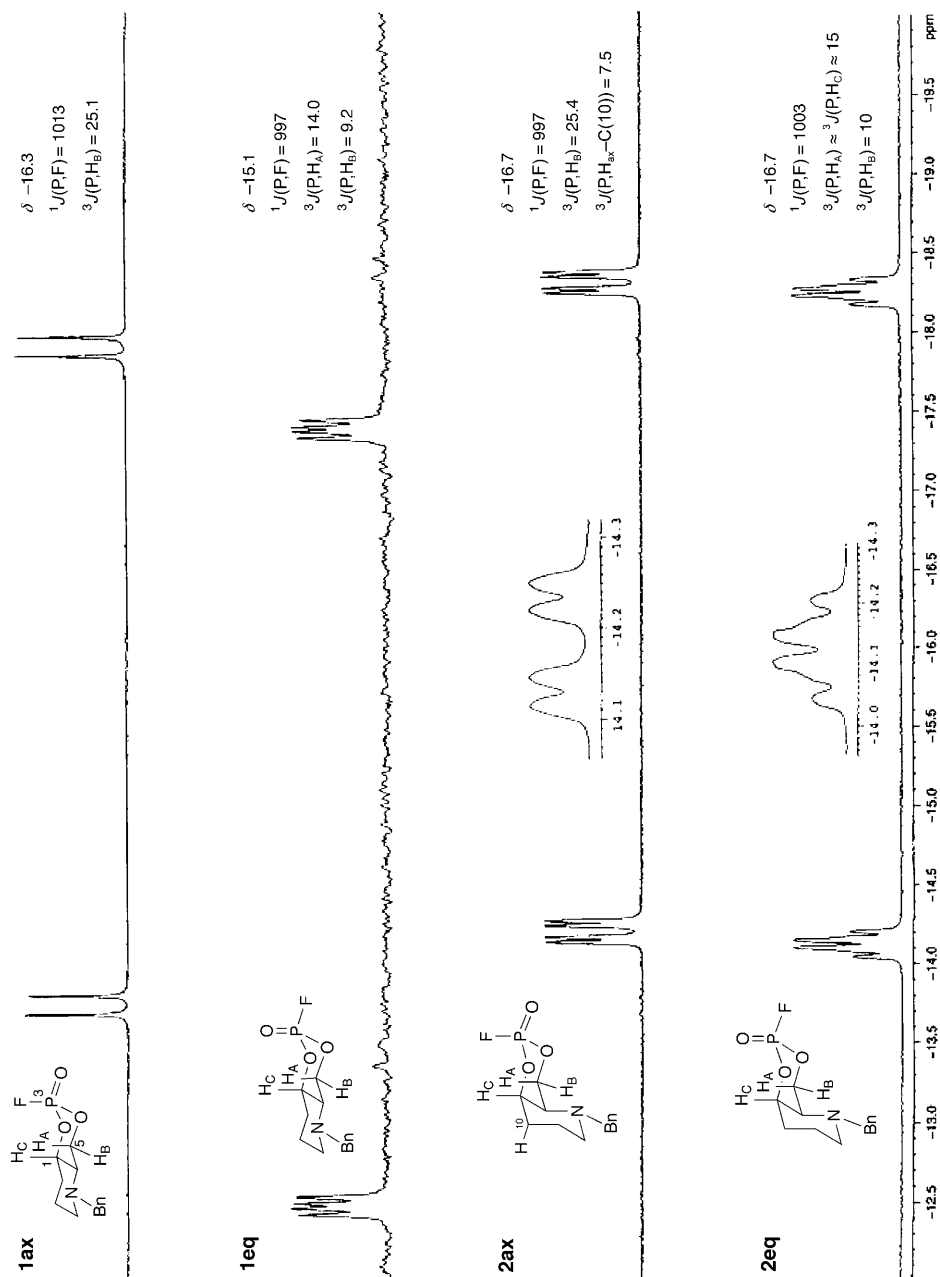
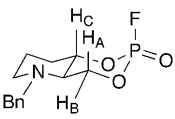
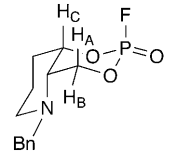


Fig. 3. ^{31}P -NMR Spectra (CDCl_3 , 242.9 MHz, 293 K) of the 2,4-dioxo-7-aza-3-phosphadecalins **1ax**, **1eq**, **2ax**, and **2eq**

Table 1. Theoretical and Experimental Conformational Data for **1ax** and **2ax**

		H _A	H _B	H _C	
	1ax: C-1	Φ [°] (Model)	60	180	60
		$^3J(\text{P,H})$ [Hz] (<i>Karplus</i>)	1	25	1
		Φ [°] (X-Ray)	71	173	65
		$^3J(\text{P,H})$ [Hz] (NMR)	1.1	25.1	0
	2ax: C-1	Φ [°] (X-Ray)	62	180	68
		$^3J(\text{P,H})$ [Hz] (NMR)	1.5	25.4	0

crystallographic (see *Sect. 4*) and the NMR data, the correlation between the dihedral angles (Φ)⁴ and the vicinal couplings of the P-atom with H_A, H_B, and H_C⁵) can be determined at six definite positions (*Table 1*)⁶. The resulting data were fitted⁷) to the general *Karplus* equation [10] to yield the customized *Eqn. 1* (*Fig. 4*). Since the crystal structure (see *Sect. 4*) and the theoretically predicted vicinal coupling data are consistent, it can be concluded that the 2,4-dioxa-3-phospha moiety in **1ax** and **2ax** adopts a chair conformation in solution, *i.e.*, **C-1**)⁵) (*Table 1*).

$$^3J_{\text{PH}}(\Phi) = \alpha \cos^2 \Phi + \beta \cos \Phi + \gamma \quad (1)$$

$$\alpha = 14.8; \beta = -8.8; \gamma = 1.8$$

3.2.2. *Conformations of the trans-Equatorial Epimer 1eq*. Generally, the steric and the stereoelectronic effects are opposite in the P(3)-equatorially substituted decalins. Although the chair conformation is sterically favored, the anomeric preference of the F-substituent to move into an axial position results in nonchair conformations

⁴) The crystallographic data are rounded and the algebraic signs of Φ are not specified as they cancel each other out by application of the *Karplus* equation (for the accurate values see *Exper. Part, Table 8*).

⁵) H_A = H_{ax}-C(5), H_B = H_{eq}-C(5), and H_C = H_{ax}-C(1). The descriptors 'ax' and 'eq', resp. are based on their relative positions in the chair conformation of the 2,4-dioxa-3-phospha moiety. Since these are not maintained in other conformational arrangements, the indices A–C are used (H_A is always *cis* to H_C). According to IUPAC conventions, the following short forms for conformations are used: **C** = chair, **B** = boat, **TB** = twist-boat, and **E** = envelope.

⁶) The absolute values of the $^3J(\text{P,H})$ were taken from the ¹H-NMR spectra, either directly, or in cases of overlapping of H_B and H_C from the ¹H,¹H-COSY. They were identified by comparison with ¹H{³¹P}-NMR spectra. Although the vicinal couplings are observable in the ³¹P-NMR (*Fig. 3*), unambiguous assignments are not possible; moreover, $^3J(\text{P,H}) < 2$ Hz are not resolved due to line broadening.

⁷) The parameters α , β , and γ were calculated by *Origin*TM 5.0 (www.microcal.com) and exhibit a dependency (quality factor) of 0.99 (α) and 0.98 (β , γ).

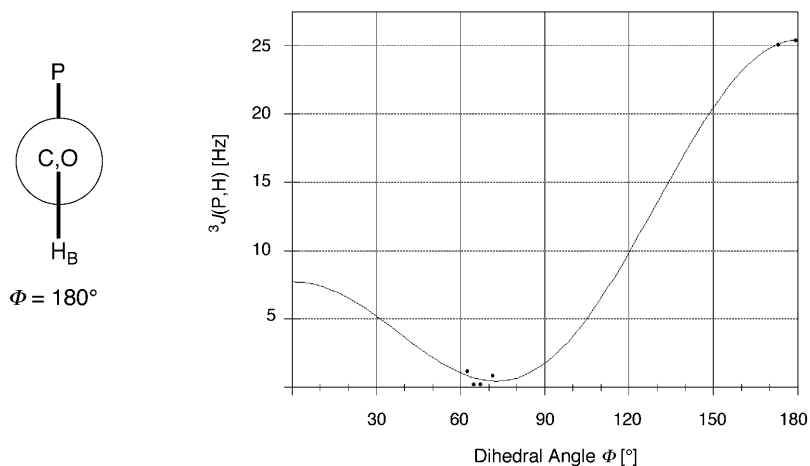


Fig. 4. The modified Karplus Equation, fitted according to the X-ray and NMR data for the double-chair conformation

such as boat or twist-boats, *i.e.*, **B**, **TB-1**, and **TB-2**⁵⁾ (Table 2)⁸⁾. To interpret the coupling patterns (Fig. 3), the torsion angles (Φ)¹⁾⁹⁾ of the decisive conformations¹⁰⁾¹¹⁾ were approximately determined with the aid of *Dreiding* molecular models and the theoretical $^3J(\text{P,H})$ calculated from Eqn. 1 (Table 2).

However, the experimental coupling data do not fit any of the depicted conformers (Table 3) and, particularly, **B** and **TB-1** can be excluded ($^3J(\text{P,H}_C) \approx 0$). Obviously, $^3J(\text{P,H}_A)$ and $^3J(\text{P,H}_B)$ are averaged, and it was assumed that **TB-2** and **C-1** are coexisting in an equilibrium mixture¹²⁾ (Table 3). This hypothesis was corroborated by variable-temperature NMR experiments that resulted in decreasing $^3J(\text{P,H}_B)$, whereas $^3J(\text{P,H}_A)$ increased upon lowering the temperature (Table 4). While $^3J(\text{P,H}_C) \approx 0$, $^3J(\text{P,H}_B)$ is a good measure for the relative proportions of **C-1** (P_{Chair}) and **TB-2** (P_{TB}) in the *trans*-2,4-dioxa-3-phosphadecalin series, the fractions can be calculated according

⁸⁾ Because the two-dimensional projections do not reflect the correct geometry, molecular models are essential to follow the reasoning.

⁹⁾ Although the *Dreiding* molecular models represent the geometry of the chemical bonds almost perfectly, some discrepancies exist between the torsion angles taken from the crystal-structure data and those derived from the molecular models. This is due to the fact that the covalent radii are not considered truly, in particular the dsp^3 -hybridized P-atom is not tetrahedral (see also Footnote 1). However, for the attempted qualitative examinations (*i.e.*, assignment or exclusion of conformations based on NMR data), the accuracy is adequate.

¹⁰⁾ According to the crystal structures (see Sect. 4) and because of the lack of anomeric preferences, the piperidine moiety is assumed to adopt a chair conformation in solution with the *N*-benzyl group in an equatorial position.

¹¹⁾ The energetically unfavored half-chair conformations were not considered.

¹²⁾ Since the spectra are well resolved and coalescence phenomena were not observed, the interconversion **C-1** \rightleftharpoons **TB-2** must be fast on the NMR time scale.

Table 2. Conformational Data for the 2,4-Dioxa-3-phospha Moiety in **1eq** and **2eq** as Determined by Dreiding Molecular Models (Φ) and Calculations from Eqn. 1 ($^3J(\text{P,H})$). As the piperidine ring does not influence the qualitative considerations, the values are identical in the *trans*-(depicted) and in the *cis*-series. **C-2** is the only additional conformation in the *cis*-series.

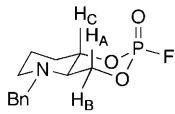
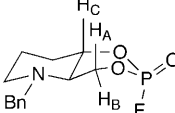
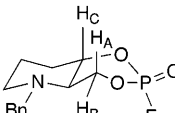
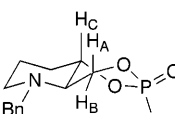
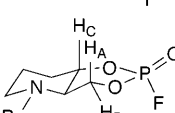
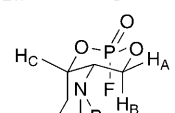
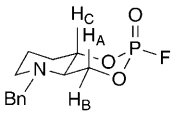
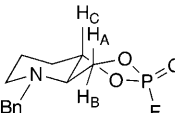
			Φ [°] (Model)	$^3J(\text{P,H})$ [Hz] (Karplus)
	1eq: C-1	H _A	60	1
		H _B	180	25
		H _C	60	1
	1eq: B	H _A	120	10
		H _B	120	10
		H _C	120	10
	1eq: TB-1	H _A	60	1
		H _B	180	25
		H _C	180	25
	1eq: TB-2	H _A	150	20
		H _B	90	2
		H _C	90	2
	1eq: E	H _A	90	2
		H _B	150	20
		H _C	90	2
	2eq: C-2	H _A	180	25
		H _B	60	1
		H _C	180	25

Table 3. Conformations of **1eq** in Solution

			H _A	H _B	H _C	
	C-1	$^3J(\text{P,H})$ [Hz] (NMR)	14	9.2	0	
				TB-2	Φ [°] (X-Ray: TB-2)	139
			$^3J(\text{P,H})$ [Hz] (Karplus)	17	4.2	1

to Eqns. 2 and 3 [10] [13]¹³). The results¹⁴) clearly indicate that by lowering the temperature, **1eq** tends to adopt the thermodynamically significantly stabilized **TB-2** conformation (Table 4)¹⁵), i.e., at sufficiently low temperatures, **TB-2** will freeze out.

$$P_{\mathbf{C}} + P_{\mathbf{TB}} \quad (2)$$

$${}^3J(\text{P,H}_{\mathbf{B}})_{\text{obs}} = {}^3J(\text{P,H}_{\mathbf{B}})_{\mathbf{C}} \cdot P_{\mathbf{C}} + {}^3J(\text{P,H}_{\mathbf{B}})_{\mathbf{TB}} \cdot P_{\mathbf{TB}} \quad (3)$$

Table 4. Low-Temperature ¹H-NMR Experiments with **1eq**

T [K] (solvent)	³ J(P,H) _{obs} [Hz]			P _{C-1} [%]	P _{TB-2} [%]	K _{eq}	ΔG [kJ/mol]
	H _A	H _B	H _C				
300 (CDCl ₃)	14	9.2	0	24	76	3.2	−2.9
293 (CD ₂ Cl ₂)	14.7	8.3	0	20	80	4	−3.4
213 (CD ₂ Cl ₂)	16.9	5.2	0	5	95	19	−5.2

3.2.3. Conformations of the *cis*-Equatorial Epimer **2eq**. The flexibility of the *cis*-decalin system and the P(3)-equatorial substituent render the situation significantly more complex, and additional conformations must be envisaged. In particular, the bicyclic system can undergo complete ring inversion to yield the prominent **C-2** arrangement (Table 2), which seems favored by the anomeric effect, the only drawback being the steric effect of the *N*-benzyl group. With regard to the decisive experimental ${}^3J(\text{P,H}_{\mathbf{A}}) \approx {}^3J(\text{P,H}_{\mathbf{B}}) \approx {}^3J(\text{P,H}_{\mathbf{C}}) \geq 10$ Hz (Fig. 3, Table 5), none of the conformations depicted in Table 2 can be excluded¹⁶), nor can any be assigned. Hence, we assume that **2eq** exists in solution as a complex mixture of **C-1/C-2**, and/or **TB-1/TB-2**, and probably also **B** or envelope **E**⁵) have to be considered.

Table 5. Experimental Data and Possible Conformations of **2eq** in Solution

		H _A	H _B	H _C
C-1, C-2, TB-1, TB-2, E	Φ [°] (X-Ray: E)	88	157	94
	³ J(P,H) [Hz] (Karplus)	1.5	22.4	2.5
	³ J(P,H) [Hz] (NMR)	14.5	10.4	14.5

¹³) The equations have also been applied to related molecules exhibiting ${}^3J(\text{P,H}_{\mathbf{C}}) \neq 0$, a fact that leads to errors [13]. As shown in Table 2, ${}^3J(\text{P,H}_{\mathbf{B}})$ is not suitable for a differentiation between **C-1** and **TB-1**. In [12], no differentiation was made between the two possible twist-boat conformations (**TB-1** and **TB-2**), and it was anticipated that certain compounds exist as 100% twist-boat with ${}^3J(\text{P,H}_{\mathbf{B}}) \approx 11.5$ Hz. Taking into account all three ${}^3J(\text{P,H})$, as tabulated in [13], this statement can be disproved.

¹⁴) The base values are ${}^3J(\text{P,H}_{\mathbf{B}})_{\mathbf{C}} = 25.1$ Hz (**1ax**, Table 1) and ${}^3J(\text{P,H}_{\mathbf{B}})_{\mathbf{TB}} \approx 4.2$ Hz (**1eq**, Table 3).

¹⁵) Note that the accuracy of the calculations is only controlled by the quality of the correspondence of the torsion angles in the crystal structure with those in solution; it does not depend on the approximate considerations based on the model conformations.

¹⁶) The most striking argument for the exclusion of a prominent conformation is that none of the ${}^3J(\text{P,H}) \approx 0$.

3.2.4. *Computation of the Conformational Energies of the P(3)-Equatorially Substituted Phosphadecalins 1eq and 2eq.* To characterize the conformational equilibrium mixtures further, the relative free enthalpies of the significant conformations of **1eq** and **2eq** at 298 K in the gas-phase were computed. Based on the default model conformations (Table 2), an energy minimization was performed according to the DFT theory [14][15] (Table 6)¹⁷⁾. The calculations showed that a default conformation was either proximate to an (intermediate) energy minimum, or it dropped into the energy minimum of another conformation exhibiting the respective characteristic torsion angles ($\Phi(\text{P,H})$).

Table 6. Calculated ΔG of the Conformations of the N-Methyl Analogues of **1eq** and **2eq** in the Gas Phase at 298 K

	C-1	C-2	B	TB-1	TB-2	E
1eq ΔG [kJ/mol]	0.1	–	→ TB-2	→ TB-2	0	→ TB-2
2eq ΔG [kJ/mol]	3.5	11.0	→ E	→ E	5.1	6.0

To validate the calculated and the experimental data, the conformational energies of the P(3)-equatorially substituted *trans*-decalin **1eq** were determined, too (Table 6). Only two stable conformations resulted: **C-1** with the F-substituent in an equatorial and **TB-2** with the F-substituent in a pseudoaxial orientation. However, the calculated **TB-2** conformation was rather flattened ($\Phi(\text{P,H}_A)=150^\circ$, $\Phi(\text{P,H}_B)=95^\circ$, $\Phi(\text{P,H}_C)=74^\circ$) and not as distinct as expected. The experimental finding that neither **TB-1** nor **B** represent stable conformations is corroborated by the calculation and, moreover, the **E** conformation could be ruled out definitively. The relative energies were not quite accurate, probably due to the influence of the solvent: it is known that the relative proportions of the **TB** conformations (more polar) of related bicyclic systems increase with increasing polarity of the solvent [13], and it is plausible that the environment CDCl_3 is more polar than in the gas phase (no solvent).

According to the computations, four of the six default conformations are populated in the more flexible *cis*-compound **2eq** (Table 6). As for **1eq**, **TB-1** and **B** can be excluded. However, the remaining ones did not converge to **TB-2**, although it looks quite favored in the *cis*-series ($\Phi(\text{P,H}_A)=176^\circ$, $\Phi(\text{P,H}_B)=59^\circ$, $\Phi(\text{P,H}_C)=46^\circ$), but to an **E** conformation. In addition, **C-2** with the F-substituent in the stereoelectronically favored axial position represents a stable conformation, but its proportion is difficult to estimate. In particular, the influence of the *N*-substituent that is assumed to be more pronounced with an *N*-benzyl group than with the *N*-methyl group used for the calculations¹⁷⁾ is inexplicit. Again, the relative energies do not exactly match the real values in solution, but the mixture of conformations adopted by **2eq** at room temperature can be restricted to **C-1**, **C-2**, **TB-2**, and **E**. Remarkably, both the **TB-1** and **B** conformations turned out to be unstable. It can be assumed that **B** is not populated in **1eq**

¹⁷⁾ To save CPU time, the *N*-methyl analogues of **1eq** and **2eq** were examined instead of the *N*-benzyl derivatives. The results show that this simplification is a good approximation.

or in **2eq** for steric reasons, but it remains unclear as to why **TB-1** is excluded, too. Probably the reasons are purely electronic, rather than steric.

4. Conformations in the Solid State; the X-Ray Analyses. – As expected and briefly anticipated in the sections above, both P(3)-axially substituted epimers **1ax** and **2ax** exclusively adopt the sterically and stereoelectronically favored double-chair conformation **C-1** (Figs. 5 and 7). In contrast, the P(3)-equatorially substituted compounds **1eq** and **2eq** exhibited significant conformational variations, and the conclusions based on the experimental data in solution were fully corroborated. In particular, the *trans*-decalin type **1eq** exists as a neat **TB-2** (Fig. 6), whereas the *cis*-isomer **2eq** adopts the unusual **E** conformation that is typical for pentacyclic compounds: C(1) to C(5) of the 2,4-dioxa-3-phospha moiety are located in a plane with C(6) forming the tip of the envelope (Fig. 8). The crystallographic data for **1ax**, **1eq**, **2ax**, and **2eq** are summarized in Table 7 and the representative torsion angles and bond lengths in Tables 8 and 9 (see *Exper. Part*).

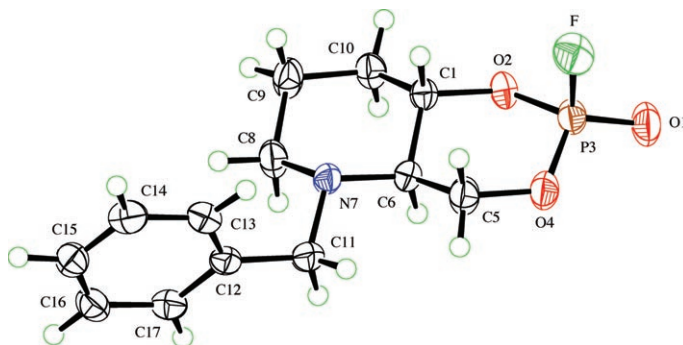


Fig. 5. The molecular structure of **1ax**. Systematic atom numbering; 50% probability ellipsoids.

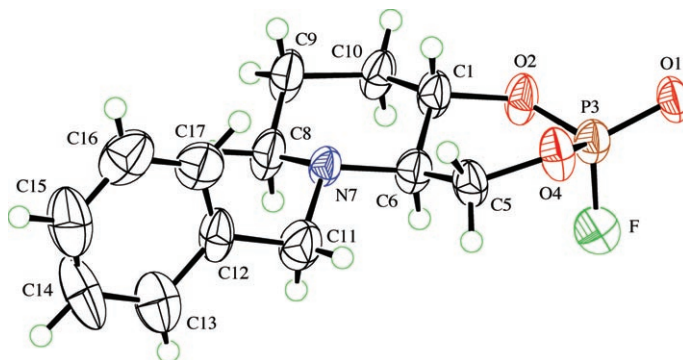


Fig. 6. The molecular structure of **1eq**. Systematic atom numbering; 50% probability ellipsoids.

5. Remarks. – This report constitutes the first direct evidence of the anomeric effect in the *cis*- and *trans*-2,4-dioxa-3-phosphabicyclo[4.4.0]decane 3-oxide series. It is based on independent comparisons of the conformations in both solution and the solid state

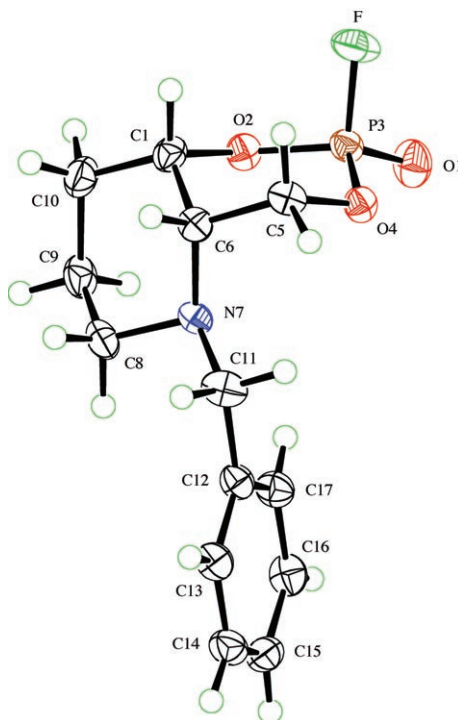


Fig. 7. The molecular structure of **2ax**. Systematic atom numbering; 50% probability ellipsoids.

by molecular-model considerations, NMR experiments, and computational and crystallographic data. Except for the crystal-structure analyses, the applied methods are not highly refined, nevertheless, they furnished reliable data, and the accuracy of the simple approaches is remarkable¹⁵). In particular, the correlation between the low-temperature ¹H-NMR experiments on **1eq** and the frozen-out twist-boat structure of the crystal-structure analysis has to be highlighted, as well as the computed convergency of the mixture of conformers of **2eq** to the unexpected, unusual envelope-type as found in the solid state.

The key parameters associated with the anomeric effect are the interatomic distances between the anomeric centre and the heteroatoms. Based on general theoretical considerations [3], an axial P–F bond is expected to be longer than an equatorial one. This was verified in our axial epimers, where the anomeric stabilization is fully operative: 1.548(1) (**1ax**), 1.528(3) (**1eq**), 1.558(1) (**2ax**), and 1.547(1) Å (**2eq**) (see Table 9, *Exper. Part*). In addition, the IR stretching frequency of an axial P=O group ($\tilde{\nu}(\text{P}=\text{O})$) was found to be *ca.* 20–30 cm⁻¹ lower with respect to an equatorial one [9][13] due to the elongated P=O bond of the former. This holds for our compounds too, as shown by the respective $\tilde{\nu}(\text{P}=\text{O})$: 1335 (**1ax**), 1292 (**1eq**), 1325 (**2ax**), and 1299 cm⁻¹ (**2eq**) [1].

The $n \rightarrow \sigma^*$ electron-donating influence of the heteroatoms X in the general arrangement X–Y–X is well understood when Y=C. Although the orbital situation is more complex when Y=P, the same arguments have been adopted unchanged [3].

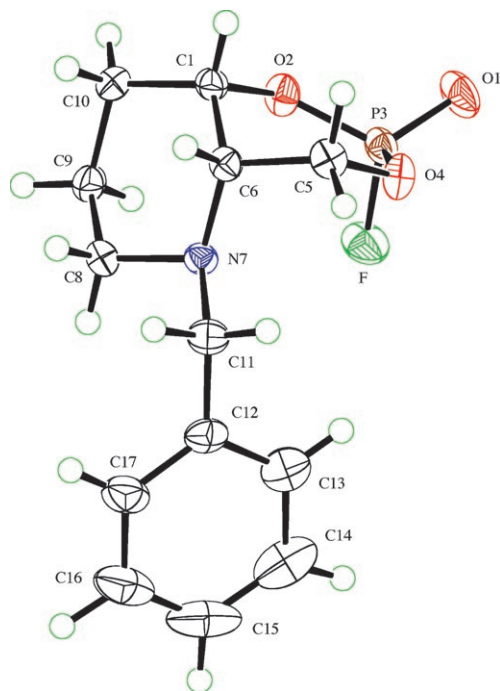


Fig. 8. The molecular structure of **2eq**. Systematic atom numbering; 50% probability ellipsoids.

However, it is highly probable that the presence of multiple lone-electron pairs and antibonding orbitals around the P-atom (d-orbitals) leads to additional contributions to the anomeric effect. Hence, it is a rather complex balance between stereoelectronic effects involving both the ester P–O and the P=O O-atom. Recently, this question became significant in the discussion of the conformational properties of the N3'-phosphoramidate backbone in DNA [16].

In the current literature, only a few crystal structures of related P(3)-substituted decalin-type organophosphates have been reported: axial *trans*-3-phenoxy-2,4-dioxo-3-phosphabicyclo[4.4.0]decane 3-oxide [17], axial *trans*-3-(2,4-dinitrophenoxy)-2,4-dioxo-3-phosphabicyclo[4.4.0]decane 3-oxide [11] and equatorial *trans*-3-(4-methoxyphenoxy)-2,4-dioxo-3-phosphabicyclo[4.4.0]decane 3-oxide [11]. In connection with research on cyclophosphamide type anticancer drugs, a crystal structure of the equatorial *trans*-*N,N*-bis(2-chloroethyl)-2-oxa-4-aza-3-phosphabicyclo[4.4.0]decane-3-amine 3-oxide [18] and a comprehensive conformational study of 3-substituted *cis*- and *trans*-4-oxa-2-aza-3-bicyclo[4.4.0]decanes has been published [19]. Remarkably, all of the reported compounds adopt the double-chair conformation in the crystal, even the P(3)-equatorially substituted congeners¹⁸⁾. This can be explained by the fact that the

¹⁸⁾ According to ¹H-NMR, the P(3)-equatorial *trans*-3-(4-methoxyphenoxy)-2,4-dioxo-3-phosphadecalin exists as a mixture of chair and twist-boat conformations (*ca.* 1:1 in CDCl₃) [11], and partially skewed conformations were assigned to a few phosphoramidates in solution [19].

substituents are electron donors, and the anomeric effect is not a determining factor. Apart from the results presented in this report, no X-ray crystallographic analyses exist of related bicyclic compounds with electron withdrawing equatorial substituents at P(3) nor have twist-boat and envelope conformations ever been completely described¹⁹).

The authors are indebted to the *Swiss National Foundation* for financial support, to Dr. *Dimitri N. Laikov* who kindly made his DFT software *Priroda* available to us, and to Dr. *Markus Furegati* for the calculations of the energies of conformations.

Experimental Part

1. *General.* See [1]. For the syntheses of the phosphadecalins, see [1]. ¹H-, ¹⁹F-, and ³¹P-NMR: *Bruker-DRX-600* (600.0, 242.9, 564.5 MHz, resp.) spectrometers; chemical shifts δ in ppm, with Me₄Si as internal or CFCl₃ and H₃PO₄ (85% in D₂O) as external standards (=0.00 ppm).

2. *Computations.* They are based on a modified DFT (density functional theory) procedure enabling a fast and sufficiently accurate evaluation of both *Coulomb* and exchange-correlation terms by using the expansion of molecular electron density in auxiliary basis sets. The approach is *ca.* an order of magnitude faster than the usual methods in which only *Coulomb* terms are treated by using the approximate density. Auxiliary basis sets of moderate size are sufficient to achieve good accuracy of molecular properties such as geometries and energies [14].

3. *X-Ray Crystal-Structure Determinations of 1ax, 1eq, 2ax, and 2eq*²⁰). All measurements were conducted at low-temperature on a *Rigaku-AFC5R* diffractometer with graphite-monochromated MoK α radiation (λ 0.71069 Å) and a 12 kW rotating anode generator. The data collection and refinement parameters are compiled in *Table 7*, selected torsion angles in *Table 8*, and representative interatomic distances in *Table 9*. Views of the molecules are shown in *Figs. 5–8*. The intensities were collected by using $\omega/2\theta$ scans. Three standard reflections, which were measured after every 150 reflections, remained stable throughout each data collection. The intensities were corrected for *Lorentz* and polarization effects, and for **2eq**, an empirical absorption correction, based on azimuthal scans of several reflections [25], was also applied. Each structure was solved by direct methods with either SHELXS97 [26] or SIR92 [27]. The non-H-atoms were refined anisotropically. The H-atoms for **1eq** were fixed in geometrically calculated

¹⁹) For the sake of completeness, it has to be mentioned that several X-ray crystallographic analyses of similar bicyclic phosphonates exist, e.g.: *cis*-equatorial and *trans*-axial 2-benzyl-3-phenyl-2-aza-4-oxa-3-phosphabicyclo[4.4.0]decane 3-oxides [20], *trans*-equatorial and *trans*-axial 4-benzyl-3-ethyl-5,5-dimethyl-4-aza-2-oxa-3-phosphabicyclo[4.4.0]decane 3-oxides, *trans*-equatorial 3,4-dibenzyl-5,5-dimethyl-4-aza-2-oxa-3-phosphabicyclo[4.4.0]decane 3-oxide, and *trans*-axial 4-[(*S*)-1,2-diphenylethyl]-3-ethyl-5,5-dimethyl-4-aza-2-oxa-3-phosphabicyclo[4.4.0]decane 3-oxide [21]. The P(3)-equatorially 3-ethyl- or 3-phenyl-substituted compounds adopt flattened [20] or slightly distorted chair conformations [21], and the 3-benzyl-substituted compound exists as a flattened half-chair [21]. In all of these compounds, the steric effects of the bulky substituents are decisive, whereas stereoelectronic effects are not operative. The same holds for the unusual boat conformation in a six-membered phosphonate (*cis*-1-(*tert*-butyl)-2,6-dioxa-1-phosphacyclohexane 1-oxide [22]) and the twist-boat evidenced in a related phosphoramidate (*cis*-*N,N*-dimethyl-2-aza-6-oxa-1-phosphacyclohexan-1-amine 1-oxide [23]). Probably the best example of dominating stereoelectronic effects in related systems is *trans*-1-methoxy-4-(*tert*-butyl)-2,6-dioxa-1-phosphacyclohexane 1-oxide [24]. This compound exists in the chair conformation with an unexpected diaxial alignment of both the 1-methoxy and the 4-(*tert*-butyl) substituent.

²⁰) CCDC-261785–CCDC-261788 contain the supplementary crystallographic data for this paper. These data can be obtained free of charge from the *Cambridge Crystallographic Data Centre*, via www.ccdc.cam.ac.uk/data_request/cif.

Table 7. Crystallographic Data for Compounds **1ax**, **1eq**, **2ax**, and **2eq**

	1ax	1eq	2ax	2eq
Crystallized from	Et ₂ O/hexane	CHCl ₃	Et ₂ O/hexane	Et ₂ O/hexane
Empirical formula	C ₁₃ H ₁₇ FNO ₃ P	C ₁₃ H ₁₇ FNO ₃ P	C ₁₃ H ₁₇ FNO ₃ P	C ₁₃ H ₁₇ FNO ₃ P
<i>M_r</i>	285.25	285.25	285.25	285.25
Crystal color, habit	colorless, prism	colorless, plate	colorless, prism	colorless, plate
Crystal dimensions [mm]	0.45×0.45×0.48	0.17×0.45×0.48	0.20×0.30×0.40	0.12×0.45×0.50
Temperature [K]	173(1)	173(1)	173(1)	173(1)
Crystal system	monoclinic	monoclinic	orthorhombic	monoclinic
Space group	<i>P</i> 2 ₁ / <i>c</i>	<i>P</i> 2 ₁ / <i>c</i>	<i>Pca</i> 2 ₁	<i>P</i> 2 ₁ / <i>c</i>
<i>Z</i>	4	4	4	4
Reflections for cell determination	25	25	24	25
2θ range for cell determination [°]	38–40	37–40	37–40	39–40
Unit cell parameters:				
<i>a</i> [Å]	7.458(2)	12.526(5)	13.276(2)	11.716(2)
<i>b</i> [Å]	17.175(2)	9.485(5)	6.546(2)	7.596(2)
<i>c</i> [Å]	10.802(2)	13.180(3)	15.791(1)	15.493(3)
β [°]	94.40(1)	116.72(2)	90	93.94(1)
<i>V</i> [Å ³]	1379.7(4)	1398.6(9)	1372.4(4)	1375.7(4)
<i>D_x</i> [g cm ⁻³]	1.373	1.355	1.381	1.377
μ(MoK _α) [mm ⁻¹]	0.214	0.211	0.215	0.215
2θ _(max) [°]	60	55	60	55
Total reflections measured	4431	3564	5322	3552
Symmetry-independent reflections	4015	3216	4004	3150
Reflections used (<i>I</i> > 2σ(<i>I</i>))	3142	2007	3241	2283
Parameters refined	241	173	240	241
Final <i>R</i> (<i>F</i>)	0.0423	0.0727	0.0359	0.0414
<i>wR</i> (<i>F</i>)	0.0425	0.0642	0.0296	0.0370
Goodness-of-fit	2.255	3.111	1.488	1.834
Secondary extinction coefficient	9(1) · 10 ⁻⁷	5(1) · 10 ⁻⁷	4.3(6) · 10 ⁻⁷	5.4(9) · 10 ⁻⁷
Final Δ _{max} / σ	0.0003	0.0001	0.0003	0.0004
Δρ (max; min) [e Å ⁻³]	0.33; -0.38	0.39; -0.33	0.24; -0.34	0.28; -0.40
σ(<i>dC</i> -C) [Å]	0.002–0.003	0.005–0.008	0.003	0.003–0.005
P–F [Å]	1.548(1)	1.528(3)	1.558(1)	1.547(1)
P=O [Å]	1.445(1)	1.451(2)	1.450(1)	1.453(2)

Table 8. Representative Torsion Angles Φ(P,H) [°]^a

	1ax	1eq	2ax	2eq
P(3)–O(2)–C(1)–H(C)	65(9)	81	68(1)	94(1)
P(3)–O(4)–C(5)–H(B)	173(1)	102	-180(1)	157(1)
P(3)–O(4)–C(5)–H(A)	-71(1)	-139	-62(1)	-88(1)

^a) H(A)=H(52), H(B)=H(51), H(C)=H(1), cf. Table 2 and Figs. 5–8.

positions (*d*(C–H)=0.95 Å), and they were assigned fixed isotropic displacement parameters with a value equal to 1.2*U*_{eq} of the parent C-atom. For all other compounds, the H-atoms were located in difference electron density maps, and their positions were allowed to refine together with individual isotropic displacement parameters. Corrections for secondary extinction were applied. The refinement of each structure was carried out on *F* by using full-matrix least-squares procedures which minimized the func-

Table 9. Representative Interatomic Distances [\AA]

	1ax	1eq	2ax	2eq
P(3)–F	1.548(1)	1.528(3)	1.558(1)	1.547(1)
P(3)–O(1)	1.445(1)	1.451(3)	1.450(1)	1.453(2)
P(3)–O(2)	1.556(1)	1.545(3)	1.552(1)	1.546(2)
P(3)–O(4)	1.552(1)	1.549(3)	1.562(1)	1.553(2)
O(2)–C(1)	1.477(2)	1.485(4)	1.480(2)	1.480(2)
O(4)–C(5)	1.472(2)	1.479(4)	1.468(2)	1.466(3)

tion $\Sigma w(|F_o| - |F_c|)^2$, where $w = [\sigma^2(F_o) + (0.005F_o)^2]^{-1}$. For **2ax** the space group is noncentrosymmetric, but requires that the compound in the crystal is racemic. The absolute structure was confirmed by refinement of the absolute-structure parameter [28][29], which yielded a value of $-0.13(6)$. Neutral-atom scattering factors for non-H-atoms were taken from [30], and the scattering factors for H-atoms were taken from [31]. Anomalous dispersion effects were included in F_{calc} [32]; the values for f' and f'' were those of [33]. The values of the mass-attenuation coefficients were taken from [34]. All calculations were performed by using the teXsan crystallographic-software package [35], and the crystallographic diagrams were drawn using ORTEPII [36].

REFERENCES

- [1] S. Furegati, W. Ganci, F. Gorla, U. Ringeisen, P. Rüedi, *Helv. Chim. Acta* **2004**, *87*, 2629.
- [2] S. Furegati, F. Gorla, A. Linden, P. Rüedi, *Chem. Biol. Interactions* **2005**, *157–158*, 415.
- [3] A. J. Kirby, 'The Anomeric Effect and Related Stereoelectronic Effects at Oxygen', Springer-Verlag, New York, 1983; D. G. Gorenstein, *Chem. Rev.* **1987**, *87*, 1047; P. P. Graczyk, M. Mikolajczyk, 'Anomeric Effect: Origin and Consequences', in 'Topics in Stereochemistry, Vol. 21', Eds. E. L. Eliel, S. H. Wilen, Wiley, New York, 1994, p. 159; I. Fleming, 'Frontier Orbitals and Organic Chemical Reactions', Wiley, New York, 1998.
- [4] W. Ganci, E. J. M. Meier, F. Merckling, G. Przibille, U. Ringeisen, P. Rüedi, *Helv. Chim. Acta* **1997**, *80*, 421.
- [5] S. Furegati, W. Ganci, G. Przibille, P. Rüedi, *Helv. Chim. Acta* **1998**, *81*, 1127.
- [6] M. J. Stöckli, P. Rüedi, *Helv. Chim. Acta* **2001**, *84*, 106.
- [7] S. Furegati, O. Zerbe, P. Rüedi, *Chem. Biol. Interactions* **2005**, *157–158*, 418.
- [8] D. G. Gorenstein, *J. Am. Chem. Soc.* **1977**, *99*, 2254, and refs. cit. therein.
- [9] D. G. Gorenstein, R. Rowell, *J. Am. Chem. Soc.* **1979**, *101*, 4925, and refs. cit. therein.
- [10] D. G. Gorenstein in 'Phosphorus-31 NMR', Ed. D. G. Gorenstein, Academic Press, Orlando, 1984; 'Phosphorus-31 NMR Spectroscopy in Stereochemical Analysis, Methods in Stereochemical Analysis Vol. 8', Eds. J. G. Verkade, L. D. Quin, Verlag Chemie, Weinheim, 1987; W. G. Bentrude, in 'Phosphorus-31 NMR Spectral Properties in Compound Characterization and Structural Analysis', Eds. L. D. Quin, J. G. Verkade, VCH Publishers, New York, 1994.
- [11] R. O. Day, D. G. Gorenstein, R. R. Holmes, *Inorg. Chem.* **1983**, *22*, 2192.
- [12] F. A. Merckling, P. Rüedi, *Tetrahedron Lett.* **1996**, *37*, 2217; F. A. Merckling, ^{31}P -NMR-spektroskopische Untersuchungen der Inhibierung von Acetylcholinesterase mit Organophosphaten', Ph.D. Thesis, University of Zurich, 1993.
- [13] D. G. Gorenstein, R. Rowell, J. Findlay, *J. Am. Chem. Soc.* **1980**, *102*, 5077.
- [14] D. N. Laikov, *Chem. Phys. Lett.* **1997**, *281*, 151.
- [15] J. P. Perdew, K. Burke, M. Ernzerhof, *Phys. Rev. Lett.* **1996**, *77*, 3865; J. P. Perdew, K. Burke, M. Ernzerhof, *Phys. Rev. Lett.* **1997**, *78*, 1396.
- [16] N. K. Banavali, A. D. MacKerell Jr., *J. Am. Chem. Soc.* **2001**, *123*, 6747, and refs. cit. therein.
- [17] P. Van Nuffel, A. T. H. Lensa, H. J. Geise, *Bull. Soc. Chim. Belg.* **1982**, *91*, 43.
- [18] J.-C. Yang, D. O. Shah, N. U. M. Rao, W. A. Freeman, G. Sosnovsky, D. G. Gorenstein, *Tetrahedron* **1988**, *44*, 6305.

- [19] H. Kivelä, Z. Zalán, P. Tähtinen, R. Sillanpää, F. Fülöp, K. Pihlaja, *Eur. J. Org. Chem.* **2005**, 1189, and refs. cit. therein.
- [20] R. J. Goodrich, T. W. Hambley, D. D. Ridley, *Aust. J. Chem.* **1986**, 39, 591.
- [21] R. Pedrosa, A. Perez-Encabo, R. Gallegos, *Synlett* **2004**, 1300.
- [22] R. O. Day, W. G. Bentrude, K. C. Yee, W. N. Setzer, J. A. Deiters, R. R. Holmes, *J. Am. Chem. Soc.* **1984**, 106, 103.
- [23] W. G. Bentrude, R. O. Day, J. M. Holmes, G. S. Quin, W. N. Setzer, A. E. Sopchik, R. R. Holmes, *J. Am. Chem. Soc.* **1984**, 106, 106.
- [24] R. W. Warrent, C. N. Caughlan, J. H. Harris, K. C. Yee, W. G. Bentrude, *J. Org. Chem.* **1978**, 43, 4266.
- [25] A. C. T. North, D. C. Phillips, F. S. Mathews, *Acta Crystallogr., Sect. A* **1968**, 24, 351.
- [26] G. M. Sheldrick, 'SHELXS97, Program for the Solution of Crystal Structures', University of Göttingen, Göttingen, 1997.
- [27] A. Altomare, G. Casciarano, C. Giacovazzo, A. Guagliardi, M. C. Burla, G. Polidori, M. Camalli, 'SIR92', *J. Appl. Crystallogr.* **1994**, 27, 435.
- [28] H. D. Flack, G. Bernardinelli, *Acta Crystallogr., Sect. A* **1999**, 55, 908.
- [29] H. D. Flack, G. Bernardinelli, *J. Appl. Crystallogr.* **2000**, 33, 1143.
- [30] E. N. Maslen, A. G. Fox, M. A. O'Keefe, in 'International Tables for Crystallography', Ed. A. J. C. Wilson, Kluwer Academic Publishers, Dordrecht, 1992, Vol. C, Table 6.1.1.1, p. 477–486.
- [31] R. F. Stewart, E. R. Davidson, W. T. Simpson, *J. Chem. Phys.* **1965**, 42, 3175.
- [32] J. A. Ibers, W. C. Hamilton, *Acta Crystallogr.* **1964**, 17, 781.
- [33] D. C. Creagh, W. J. McAuley, in 'International Tables for Crystallography', Ed. A. J. C. Wilson, Kluwer Academic Publishers, Dordrecht, 1992, Vol. C, Table 4.2.6.8, p. 219–222.
- [34] D. C. Creagh, J. H. Hubbell, in 'International Tables for Crystallography', Ed. A. J. C. Wilson, Kluwer Academic Publishers, Dordrecht, 1992, Vol. C, Table 4.2.4.3, p. 200–206.
- [35] 'teXsan: Single Crystal Structure Analysis Software', Version 1.10, Molecular Structure Corporation, The Woodlands, Texas, 1999.
- [36] C. K. Johnson, 'ORTEPII', Report ORNL-5138, Oak Ridge National Laboratory, Oak Ridge, 1976.

Received March 27, 2006